Parametric Study of the Flow in Printing and Coating Nips: The Influence of non-Newtonian Fluids

M.F.J. Bohan [*], I.J. Fox [*], D.T. Gethin [*] and T.C. Claypole [*]

Keywords: modelling, nip contacts, rheology, ink flow

Abstract

The changes in flow through nip contacts will significantly affect coat weight and print colour. The evaluation of the performance of printing and coating nips is a generic problem for many industrial applications. Previously this has been modelled using boundary element methods [1], [2] for Newtonian fluids. However, within these nips high shear rates are generated and these will affect the viscosity and subsequent performance of the nips for non-Newtonian fluids. A power law fluid model has been used to model the shear rate to viscosity relationship. The model results quantify the changes in pressure, film thickness and flow rate that can occur when changing the fluid properties, for example the viscosity, degree of shear thinning. It is successfully applied to a number of different system geometries.

Introduction

The transfer of fluid to a substrate using a number of hard and soft rubber covered roller is used in many lithographic and coating applications, a typical application for lithographic printing is shown in Figure 1. The mechanical configuration, fluid properties and the operating conditions determine the quantity of fluid transferred. These can use many different fluids and may operate in either rolling or sliding.

As the fluid flows through the nip contact, pressure is generated. This pressure field will lead to the deformation of the elastomeric layer and this deformation will affect the film thickness and hence the pressure in the nip contact. This

[*] Welsh Centre for Printing and Coating, University of Wales Swansea

contact is referred to as that of Soft Elasto Hydrodynamic Lubrication (Soft EHL) in a line contact.

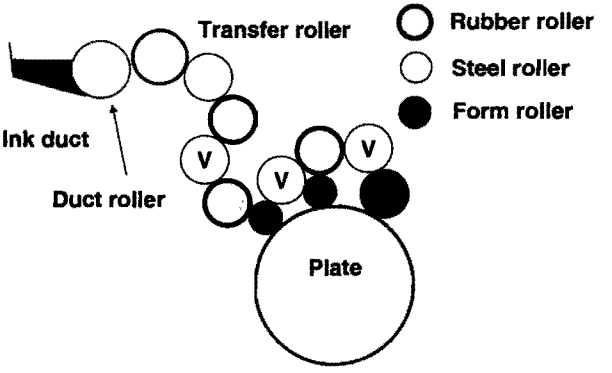

Figure 1 Typical configuration of a roller train

The evaluation of nip contacts for both hard and soft EHL has been reported in the literature, for both numerical and experimental applications. One of the first [3] provided the analysis basis for many subsequent papers and focused on dry contacts. These approaches have been developed to address plane strain [4] and evaluate parameters including the Poisson's ratio, geometry and speed [5], [6], [7]. One of the first analysis of wet contacts investigated a hard roller contacting a polythene target [8]. The methodology was improved using inlet / outlet analysis and Hertzian evaluation of the contact [9], [10].

The requirement to iterate between the elastomer and fluid regimes was first identified as an issue to be addressed in [11] and the results of the model showed the geometry to be key in the nip performance. This work was extended [12] to evaluate different inlet conditions replicating starved or flooded nips.

The application to printing and coating has occurred in recent years with the first [13] concentrating on inlet conditions and showing general agreement with the results presented in [12]. Coating applications were evaluated [14] with the sub-ambient at the exit being modelled using a Landau-Levich rupture model. The model also investigated unsteady conditions using perturbations and evaluated both cavitation and the onset of ribbing. This was extended [15] to allow the analysis of the contact using a fundamental approach, allowing the assumption of the Hertzian contact to be investigated and the results showing that the contact deviated from this form. Subsequently, parametric studies of the nip contacts have been carried out [1], [2] evaluating geometric, process and fluid properties.

Little work has been carried out evaluating the impact of non-Newtonian fluids, highlighted in [16], with the authors indicating that the major developments required were in the analysis of real systems, in terms of the fluid and the mechanics of the surface. The analysis of rolling conditions has been studied in [17], [18], in which the authors used power law fluids. The first [17] focused on non-dimensional analysis of the nip contact while the second [18] evaluated the fluid rheology and the impact of shear rate cut off and compared the results to those obtained experimentally.

The aim of the current work is to extend this to evaluate the impact of both the rheology and geometry on the nip performance for both rolling and sliding applications. The paper will quantify the impact of the shear on the local viscosity fields in the nip and then its impact on the pressure profiles and pumping capacity.

Model background

The analysis of the soft elastohydrodynamic lubrication requires the solution of both the fluid and elastomer regimes. The deformation of the elastomer will effect the pressure through the nip and as such the solution is iterative and needs to be coupled. The non-Newtonian fluid behaviour is incorporated into the solution of the generalised pressure equation. The following section outlines the background theory and the solution procedure required,

Generalised Pressure Equation

For a non-Newtonian fluid flow, the thin film equations are derived accounting for the variation of viscosity, leading to a generalised pressure equation [19]. Provided that the analysis plane is some distance from the roller edge then this equation can be written in a one-dimensional form as

$$\frac{d}{dx}\left[G\frac{dp}{dx}\right]=U_2\left[\frac{dh}{dx}\right]+(U_1-U_2)\left[\frac{dF}{dx}\right] \qquad \ldots 1$$

where

$$G=\int_o^h \frac{y}{\mu}(y-F)dy \qquad \ldots 2$$

$$F_1=\int_0^h \frac{y}{\mu}dy; F_0=\int_0^h \frac{1}{\mu}dy; F=\frac{F_1}{F_0} \qquad \ldots 3$$

The integrals can be evaluated and the pressure equation (1) solved for a non-Newtonian fluid once the variation of viscosity is known over the film thickness.

A finite difference numerical scheme was used to solve this equation. A power law equation was used to define the viscosity field using the following equation.

$$\tau = m\left|\frac{du}{dy}\right|^{n-1}\frac{du}{dy} \qquad \ldots 4$$

The term $m\left|\frac{du}{dy}\right|^{n-1}$ effectively represents the viscosity coefficient. For a Newtonian fluid n is set to 1 and m is the dynamic viscosity. When n is less than 1, the fluid adopts a shear thinning behaviour. The determination of viscosity through the film relies on the calculation of the local velocity gradient and these may be determined through numerical differentiation of the velocity profile. These also need to account for the cross film viscosity variation and therefore the velocity variation was derived using equation (5). This equation embodies the velocity boundary condition that the fluid adheres to each roller surface and therefore moves at their respective surface velocities U_1 and U_2.

$$u(\alpha) = U_1 + \frac{dp}{dx}\int_0^\alpha \frac{y}{\mu}dy + \left(\frac{U_2 - U_1}{F_0} - \frac{F_1}{F_0}\frac{dp}{dx}\right)\int_0^\alpha \frac{dy}{\mu} \qquad \ldots 5$$

This equation includes a cross film variation of viscosity in terms F, requiring it to be solved iteratively. This was implemented within the solution algorithm with a close tolerance on viscosity at each point through the film. For extreme conditions it was also necessary to introduce damping into the solution to ensure stability.

Elastic deformation

Assuming the rubber layer on the roller to be linearly elastic as there are only small deformations then for a plain strain case, the boundary element integral equation for the solution of the general problem of elastostatics is given below

$$c_{lk}^i u_k^i + \int_\Gamma p_{lk}^* u_k d\Gamma = \int_\Gamma u_{lk}^* p_k d\Gamma + \int_\Omega u_{lk}^* b_k d\Omega \qquad \ldots 6$$

However, for the problem examined, the body forces are zero with no thermal or gravitational forces and the equation (6) can be simplified to

$$c_{lk}^{i}u_{k}^{i} + \int_{\Gamma} p_{lk}^{*}u_{k}d\Gamma = \int_{\Gamma} u_{lk}^{*}p_{k}d\Gamma \qquad \ldots 7$$

Numerical singularities in the solution can occur when a field point ζ_0 is located at a node where the integration takes place. These can be eliminated with the use of corner factors and the techniques are indicated in [20], [21]. The use of linear elements in a finite plane model allows the element integrals to be calculated analytically. As well as allowing a rapid solution, this allows elements to be formulated that are suited to a solution with a Poisson's ratio of 0.5 avoiding the numerical singularity that is usually present with this material property specification.

Film Thickness

The film thickness was expressed using the following equation using an equivalent roller radius. A negative value of h_0 indicates a roller engagement and the term $u_d(x)$ represents the local deformation of the elastomer layer.

$$h(x) = h_0 + \frac{x^2}{2R} + u_d(x) \qquad \ldots 8$$

Load

The solution strategy seeks to modify the film thickness profile to satisfy a load application constraint and completion of the solution was obtained when the computed load meets the set value, to a tolerance, T_l, of less than 0.1 percent.

$$\left| \left[\int_{x_1}^{x_2} p.dx \right] - L \right| \leq T_l * L \qquad \ldots 9$$

Solution procedure

This involves the iterative solution of equations outlined above and can be summarised as

i Define the mesh over the elastomer boundary and calculate the division for the fluid side calculations.
ii Calculate the Hertzian pressure and the consequent deformation.
iii Set an initial value for the engagement, h_0.
iv Calculate the film thickness in the nip junction.
v Solve for the film pressure, including iteration for non-Newtonian behaviour.
vi Recalculate the elastomer deformation.

vii If the deformation has not met the convergence criteria, then repeat from stage (iv) with the new deformation.

viii Once the deformation criterion has been met, examine the load equilibrium. If this is not met then appoint a new value for h_0 and repeat from (iv).

The convergence requirement for the analysis was 0.1 percent on the pressure and indentation. Convergence of the solutions was usually obtained in approximately 5,000 iterations.

Model parameters

Typical industrial configurations have been used to investigate the applicability and range of the numerical model. These have been based primarily on the roller trains found in lithographic printing presses. These conditions are itemised in Table 1 (basic set), with the mechanical properties of the elastomer being obtained experimentally [22]. Typical inks have been characterised [18], [23], and these have been modelled using the power law equation. The mean values chosen for the analysis were a viscosity coefficient, (m), of 30 and a power law index, (n), of 0.75.

Parameter	Basic	Orthogonal array data Level 2
Load	2500 Nm^{-1}	
Roller radius	0.050 m	0.0625 m
Rubber thickness	0.008 m	
Rubber elastic modulus	4.0e+6 Pa	5.0e+6 Pa
Speed	1.0 ms^{-1}	1.25 ms^{-1}
Newtonian viscosity	7.54	
m	30	22.2
n	0.75	0.5625

Table 1 Parameters used for model evaluation

A shear rate cut off was used for both the upper and lower limits of the power law model, these have been used in models previously [17], [24]. The values selected were 250 s^{-1} and 4000 s^{-1}, which followed trials evaluating the sensitivity of the solution to the value used. Setting the lower value to high would have limited the effect of the shear thinning behaviour, while the higher limit is used to minimise computational time, the value not significantly affecting the model of the nip performance.

The lower shear rate cut-off of 250 s^{-1} leads to a viscosity of 7.54 Pas. This value was then used in all calculations for Newtonian fluid. Orthogonal array

methods [25], [26] were used to quantify the effects of the main process parameters on the nip performance. For each case they were altered by 25% and the values used are listed, Table 1 (orthogonal array data, level 2).

Results and discussion

The effect of the non-Newtonian power law fluid behaviour is for the viscosity to change as the shear rate alters through the nip. The shear rate and viscosity profiles for a typical printing nip are shown in Figure 2, for the conditions outlined in Table 1. The case shown is for a rolling scenario and hence the gradients are symmetrical about the middle of the fluid height (50%). The shear rate contours show a high shear rate occurring near the nip inlet and outlet, caused by the high-pressure gradients in these regions, Figure 3. These are near to the surface as Poiseulle flow component is dominant in a rolling situation. These high shear rates lead to a significant drop in the viscosity, by approximately 50%. This shows that even for the low press speeds and rolling applications large changes in the fluid viscosity occur in the nip.

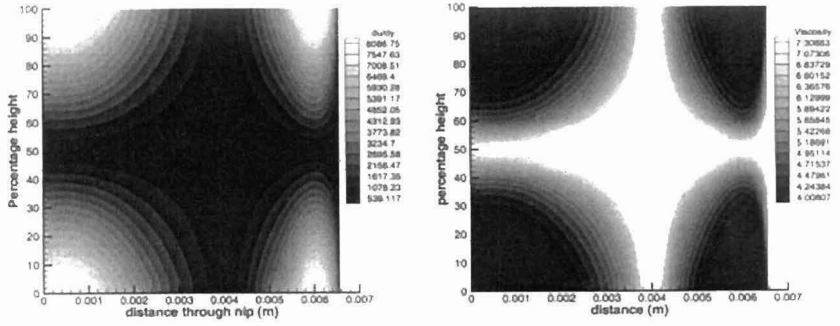

Figure 2 Shear rate and viscosity variation through the nip section m=30, n=0.75, U=1.0 m/s

The impact of changing to a non-Newtonian fluid for a rolling nip contact was initially assessed, Figure 3, the condition for the model is shown in Table 1. The impact of change in fluid properties shows a small change for the pressure profile with a much greater one in the film thickness. For the pressure profile, the small change is a result of the same contact width and the convergence criteria of constant load. The peak pressure moves towards the nip exit with an increased value. This can be explained by considering the film thickness at this point, which is much lower at this point. In addition, both fluids have similar viscosities in the middle of the nip, due to the lower shear encountered, as there are small pressure gradients only, Figure 2. The large amount of shear thinning

occurring in the nip has lead to a significant drop in the film thickness. This has a resultant affect on the flow rate in changing to a non-Newtonian fluid, for which a large drop is computed.

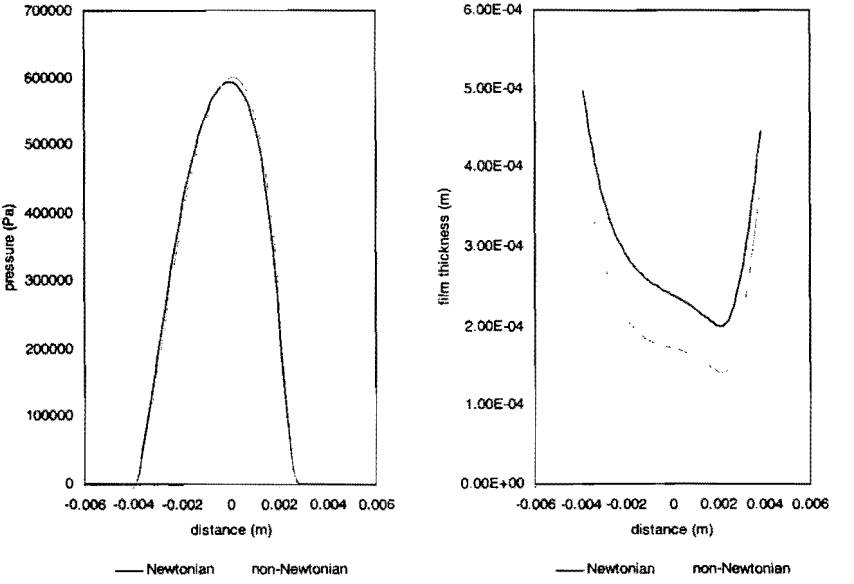

Figure 3 Influence of non-Newtonian Behaviour on the Pressure Profile and Film Thickness

The results have shown that changing to a non-Newtonian fluid has a large effect on the nip performance. The influences of the power law index (n) and viscosity coefficient (m) were investigated with the power law index was varied from 0.55 to 0.95 and the viscosity coefficient varied from 10 to 50. This covers a wide range of different ink performances commonly found in lithographic printing. The effect of the power law index is shown in Figure 4. As the value is reduced from 1, the fluid exhibits a greater degree of shear thinning. The impact on the nip is to cause the peak pressure to rise and the profile to move into the nip, as was seen when comparing the Newtonian and non-Newtonian fluids. A large change is seen in the magnitude of the film thickness profile with a greater than 80 percent drop in the minimum film thickness. This effect is non-linear and analysis of the flow rate shows this is transferred into a non-linear change in the flow rate.

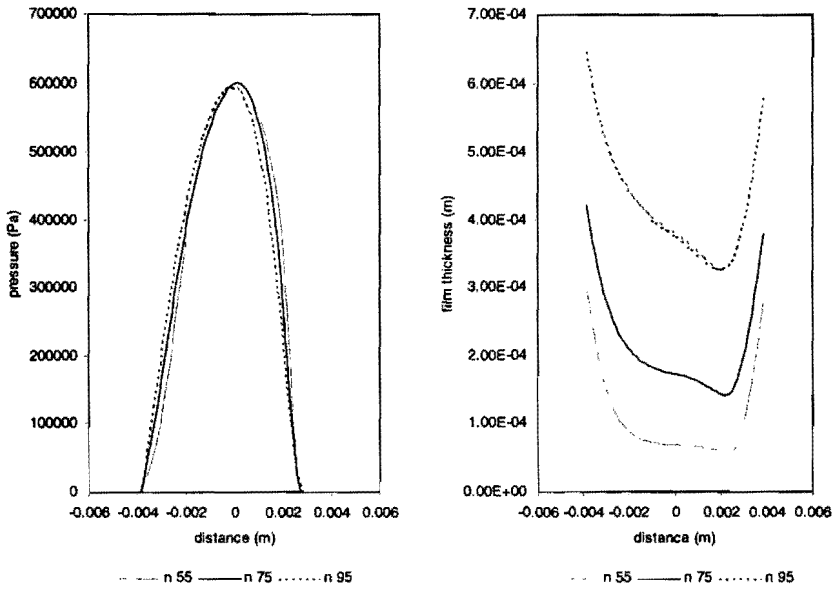

Figure 4 The influence of power law index on pressure and film thickness, U=1.0 m/s, m=30 Pas

The viscosity coefficient (m) has a large influence on the film thickness characteristics and only a small effect on the pressure profile, Figure 5. As this is increased, the initial value of the fluid viscosity increases, and can be compared to increasing the viscosity for a Newtonian fluid. In a similar manner to [2] the minimum film thickness increases as the viscosity coefficient is increased. The changes in the minimum film thickness are non-linear with a greater drop from 30 to 10 (46%) compared to that for the drop from 50 to 30 (25%). This is, in part, a function of the power law fluid model, in that at the low viscosities, as the film thickness reduces the amount of shear increases, which further reduces the minimum film thickness.

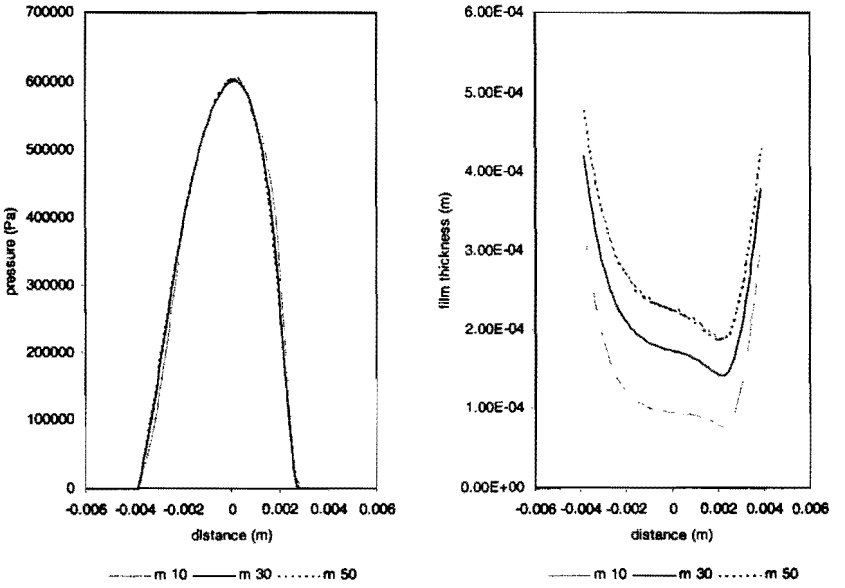

Figure 5 The influence of viscosity coefficient on pressure and film thickness, U=1.0 m/s, n=0.75

The effect of the changes in the power law coefficients on the viscosity field can be used to understand the changes that occur in the pressure and film thickness profiles. These are shown in Figure 6. As the power law index is reduced from 0.95 to 0.55 the low shear cut off reduces by an order of magnitude with the resultant reduction in the viscosity and subsequently the minimum film thickness, Figure 4. With the higher power law index, the viscosity gradients through the nip are smoother. Considering the viscosity coefficients, as these are reduced so the bulk viscosity in the nip is reduced, again with the resultant drop in the film thickness, Figure 5. With the higher viscosity, the viscosity transition within the nip is much smoother, as seen with the power law index.

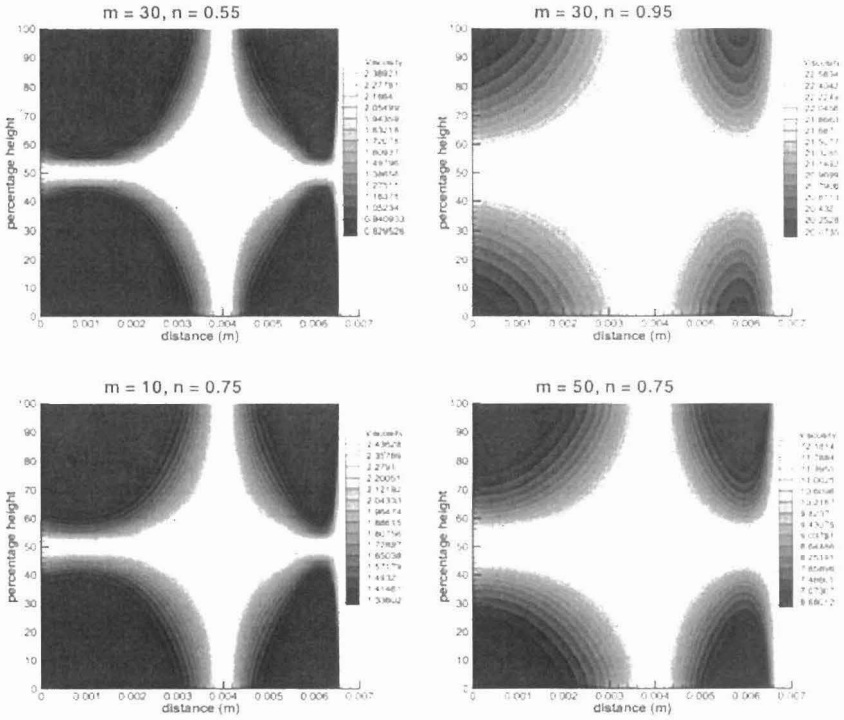

Figure 6 Shear rate and viscosity variation through the nip section for varying m and n, U=1.0 m/s

The examples discussed have all been for pure rolling. As sliding is introduced to one of the surfaces there is a small reduction in the peak pressure and shift in the profile as the higher shear results in a lower viscosity. However, the models converge on constant load and as such the changes detected are small. Large non linear changes are seen in the film thickness profile, Figure 7. The higher film thickness can be attributed to the greater entrainment at the higher speed, which results in a lower amount of shear within the nip contact, Figure 8. Considering the viscosity profiles, these show large differences from the rolling case, Figure 2, with the profiles being asymmetric. Larger portions of the nip are sheared for the sliding case, with the result that the overall viscosity in the printing nip is reduced.

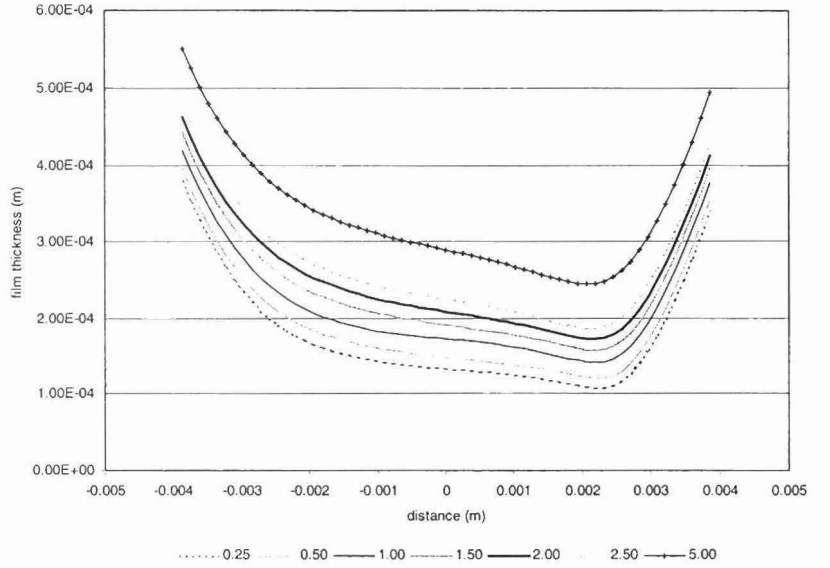

Figure 7 Influence of sliding on pressure and film thickness, U_1=1.0 m/s, m=30 Pas, n=0.75

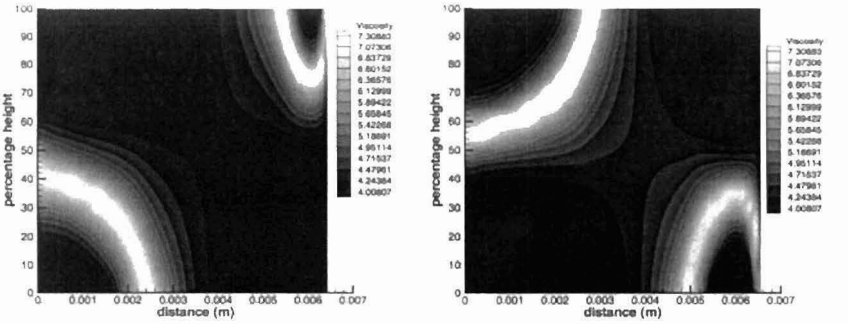

U_2 = 0.5 m/s U_2 = 1.5 m/s

Figure 8 Shear rate and viscosity variation through the nip section m=30, n=0.75

The effect of varying the elastomer modulus on the nip characteristics is shown in Figure 9. These show that as the elastomer modulus is reduced that the contact width broadens and the peak pressure is reduced, while the minimum film thickness is reduced and moves towards the centre of the nip. The contact width start point is set during the initial set-up and is dependent on the elastic modulus. As the modulus is increased the contact width reduces. The constant

load analysis then forces the increase in the maximum pressure. The reduction in the elastomer modulus lessens the stiffness and increases the deformation. As the pressure is increased this then causes a reduction in the minimum film thickness.

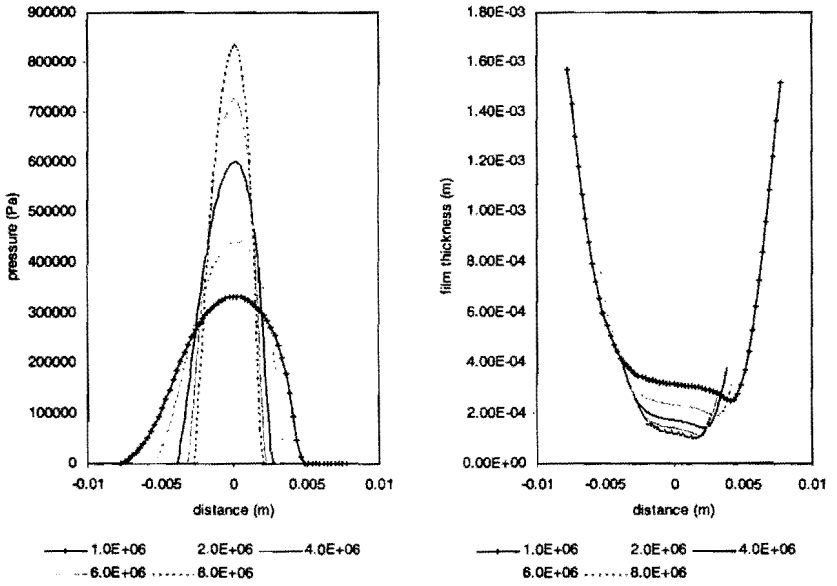

Figure 9 Influence of elastic modulus on pressure and film thickness, U_1=1.0 m/s, m=30 Pas, n=0.75

The process parameters have a large and varying influence on the flow rate through the nip, Figure 10. The data has been normalised to the conditions outlined in Table 1, to allow comparison of the flow rate information. This shows the flow is significantly affected by many of the variables, with the largest impact with the power law index (n), indicated by the highest gradient. A small increase in this results in a large increase in the flow rate as the fluid acts in a more Newtonian manner. Increasing the speed in either rolling or sliding will increase the flow through the nip as the Couette component becomes more significant. To assess the impact of the parameters individually and quantify any possible interactions orthogonal array analysis has been carried out using five of the major parameters affecting the flow rate. Analyses of several quality characteristics were made including the maximum pressure, minimum film thickness and flow rate. As the contact width varied it was not possible to plot the impact on the nip profiles. Therefore results are analysed for each of the discrete variables independently. The results show that parameters affecting the pressure profile do not necessarily affect the flow through the nip, similar to trends presented earlier [1] for Newtonian fluids. The mechanical properties

have the most effect on the pressure profile and contact width, while the minimum film thickness and flow rate were effected primarily by the fluid properties and press speed. Most changes in the nip performance were smaller than those made to the individual parameters, with the exception of the power law index (n). Here the flow rate and film thickness were very sensitive to changes, with those in the nip performance being three times greater than the change in the power law index. The implications are that for small changes in the viscosity characteristic, through contamination or supplier change, there will be a large change in the printed colour and that this will not be even through the printed product and production. Throughout the analysis no large interactions were found between the parameters.

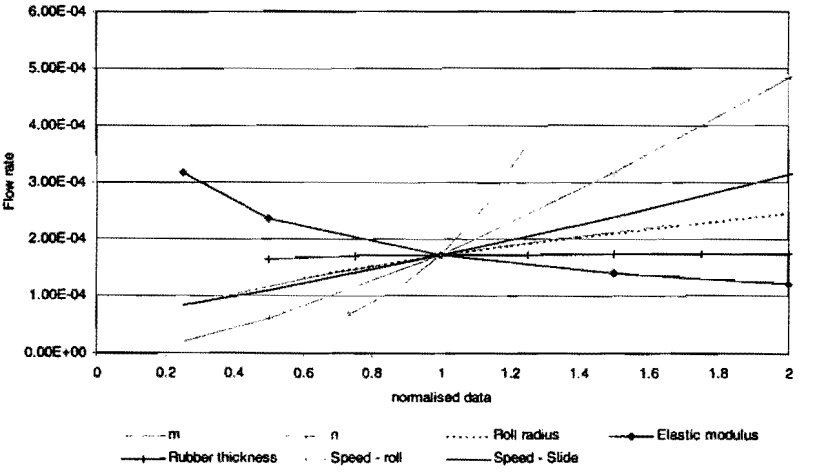

Figure 10 Change in flow rate with parameter variation, m= 30 Pas, n=0.75, roll radius = 0.050 m, elastic modulus = 4.0e+6 Pa, rubber thickness = 0.008 m, U= 1 ms^{-1}

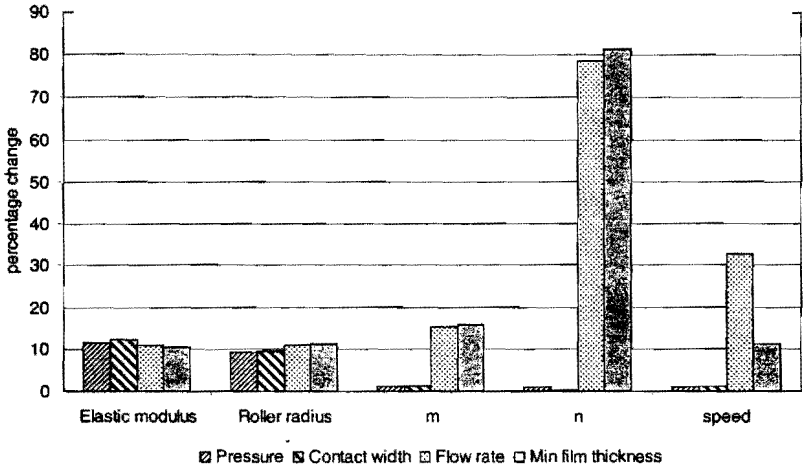

Figure 11 Parametric study into the nip performance of elastic modulus, roller radius, roller speed, power law co-efficient and index

Conclusions

A fast and computationally efficient model has been developed for a soft elastohydrodynamic lubrication contacts using a power law non-Newtonian fluid in rolling and sliding. This covers many printing and coating applications. The model couples the solution of the generalised pressure equation with those of elastostatics. The two dimensional elasticity equations possess the advantage of theoretical strictness. The model could be developed to encompass other non-Newtonian fluid models.

The impact of the non-Newtonian fluid behaviour can be summarised as

- Reducing the fluid viscosity within the nip compared to the Newtonian fluid
- As both the power law index and viscosity coefficient reduce, the nip performance changes notably
  - The peak pressure moves into the nip
  - Reduction in the film thickness
  - Reduction in the pumping capacity of the nip

The parametric study has shown that for the nip conditions

- Mechanical properties effect the maximum pressure and contact width
- All parameters analysed effected the flow rate through the nip
- Minimum film thickness is not a good indicator for changes in the flow rate
- Flow rate most sensitive to changes in the power law index
- No large interactions were found between the parameters assessed

Acknowledgements

The authors wish to acknowledge the financial support of the EPSRC platform grant programme, European Community, ELWa, Welsh Development Agency and the European Regional Development Fund.

References

1 Bohan, M.F.J., Claypole, T.C. and Gethin, D.T. "Boundary element modelling of printing and coating nips in a sliding contact" 50th TAGA Tech. Conf., Chicago, May 1998.

2 Bohan, M.F.J., Claypole, T.C., Gethin, D.T. and Basri, S.B. "Application of boundary element modelling to soft nips in rolling contact", 49th Annual TAGA Tech. Conf., Quebec City, Canada, May 1997.

3 Hannah, M. "Contact stress and deformation in a thin elastic layer", Quarterly Journal of Mechanics and Applied Maths, 4, p 94-105, 1951.

4 Parish, D.J. "Apparent slip between metal and rubber covered pressure rollers", Bri. J. Appl. Maths, Vol 9, p 428-433, 1958.

5 Miller, R.D.W., Some Effects of Compressibility on the Indentation of a Thin Elastic Layer by a Smooth Rigid Cylinder; Applied Scientific Research, 16, 1966, p 405-424.

6 Meijer, P., "The Contact Problem of a Rigid Cylinder on an Elastic Layer", Applied Scientific Research, 18, 1968, p 353-383.

7 Jaffar, M.J. and Savage, M.D. "On the Numerical Solution of Line Contact Problems Involving Bounded and Unbonded Strips", Proc. I.Mech.E. Journal of Strain Analysis, 23, 1988, p 67-79.

8 Bennett, J. and Higginson, G.R., "Hydrodynamic lubrication of soft solids", Proc. I.Mech.E. Journal of Mechanical Engineering Sciences, 12, p 218-222, 1970.

9 Hooke, C.J. and O'Donoghue, J.P., "Elastohydrodynamic lubrication of soft, highly deformed contacts", Proc. I.Mech.E., Journal of Mechanical Engineering Sciences, 14, p 34-48, 1972.

10 Gupta, P.K., "On the heavily loaded elastohydrodynamic contacts of layered solids", Trans. ASME, J. Lubric. Tech., 98, p 367-374, 1976.

11 Cudworth, C.J. "Finite Element Solution of the Elastohydrodynamic Lubrication of a Compliant Surface in Pure Sliding", 5th Leeds-Lyon Symposium on Tribology, Leeds, 1979.

12 Hooke, C.J. "The Elastohydrodynamic Lubrication of a Cylinder on an Elastomeric Layer" Wear, 111, p 83-99, 1986.

13 MacPhee, J., Shieh, J. and Hamrock, B.J. "The Application of Elastohydrodynamic Lubrication Theory to the Prediction of Conditions Existing in Lithographic Printing Press Roller Nips" Advances in Printing Science and Technology, 21, p 242-276, 1992.

14 Carvalho, M.S. and Scriven, L.E. "Deformable Roller Coating Flows: Steady State and Linear Perturbation Analysis", Journal of Fluid Mechanics, 339, 1997, p143-172.

15 Bohan, M.F.J., Lim, C.H., Korochkina, T.V., Claypole, T.C., Gethin, D.T. and Roylance, B.J. "An investigation of the hydrodynamic and mechanical behaviour of a soft nip in rolling contact", Proc. IMechE part J, vol. 211 no. J1, pp37-50, 1997.

16 Dowson, D. and Ehret, P. "Past, Present and Future Studies in Elastohydrodynamics", Proc I Mech E (J), 213, 1999, p317-333.

17 Jacobson, B.O. and Hamrock, B.J. "Non-Newtonian Fluid Model Incorporated into Elastohydrodynamic Lubrication of Rectangular Contacts" Trans. ASME (JOLT), 106, p 275-284, 1984.

18 Lim, C.H., Bohan, M.F.J., Claypole, T.C., Gethin, D.T. and Roylance, B.J. "A finite element investigation into a soft rolling contact supplied by a non-newtonian ink", J. Phys. D: Appl. Phys, vol. 29, pp 1894-1903, 1996.

19 Dowson, D. "A Generalised Reynolds Equation for Fluid Film Lubrication" International Journal of Mechanical Engineering Sciences., 4, 1962, p 159-170.

20 Brebbia, C.A. and Dominguez, J. "Boundary elements: An introductory course", McGraw Hill, 1989.

21 Banerjee, P.K. and Butterfield, R. "Boundary element method in engineering science", McGraw Hill, New York, 1981.

22 Lim, C.H. "An elastohydrodynamic behaviour of a soft printing roller nip", PhD thesis, U.W. Swansea, 1995.

23 Wildgust, P. "The Rheology of Printing Inks", M.Eng Project, UWS, 1995

24 Bohan, M.F.J., Fox, I.J., Claypole, T.C. and Gethin, D.T. "Numerical modelling of elastohydrodynamic lubrication in soft contacts using non-Newtonian fluids" in press, Int. J. Heat & Fluid Flow.

25 Phadke, M.S., "Quality engineering using robust design", 1989 (Prentice Hall Int).

26 Groove, D.M. and Davies, T.P. "Engineering quality and experimental design", Longman Sci. and Tech., 1992.

Nomenclature

b_k	body forces within boundary domain
c_{ik}^{i}	corner factor for the boundary integral equation
F_1	integral in the pressure equation
F_1	integral in the pressure equation
G	shear modulus in Kelvin solution
h	fluid film thickness
h_0	roller engagement

L	load
m	viscosity coefficient
n	power law index
p	fluid pressure
p_k	traction for the boundary integral equation
p^*_{lk}	traction for Kelvin solution
R	equivalent roller radius
U_1	roller 1 surface velocity
U_2	roller 2 surface velocity
U	velocity
u_d	surface indentation
u_k	displacement for the boundary integral equation
u^*_{lk}	displacement for Kelvin solution
x	co-ordinate for film
y	cross film height co-ordinate
Γ	boundary surface
ζ_0	point on the boundary
μ	fluid viscosity
Ω	boundary domain
τ	shear stress